

AperTO - Archivio Istituzionale Open Access dell'Università di Torino

Effect of carbon fiber type on monotonic and fatigue properties of orthopedic grade PEEK

This is the author's manuscript

Original Citation:

Availability:

This version is available <http://hdl.handle.net/2318/1688286> since 2019-01-29T11:36:26Z

Published version:

DOI:10.1016/j.jmbbm.2018.10.033

Terms of use:

Open Access

Anyone can freely access the full text of works made available as "Open Access". Works made available under a Creative Commons license can be used according to the terms and conditions of said license. Use of all other works requires consent of the right holder (author or publisher) if not exempted from copyright protection by the applicable law.

(Article begins on next page)

Effect of carbon fiber type on monotonic and fatigue properties of orthopedic grade PEEK

Keywords: PEEK composites; fatigue crack propagation; orthopedic biomaterials; fractography

Noah Bonnheim, MS (corresponding author)
Department of Mechanical Engineering, University of California, Berkeley
2121 Etcheverry Hall
Berkeley, CA 94720
noah.bonnheim@berkeley.edu
(214) 288-1730
No conflicts of interest

Farzana Ansari, PhD
Exponent, Inc.
149 Commonwealth Drive
Menlo Park, CA 94025
No conflicts of interest

Marco Regis, PhD
Department of Chemistry, Università degli Studi di Torino
Via P. giuria 7
10125 Torino Italy
No conflicts of interest

Pierangiola Bracco, PhD
Department of Chemistry, Università degli Studi di Torino
Via P. giuria 7
10125 Torino Italy
No conflicts of interest

Lisa Pruitt, PhD
Department of Mechanical Engineering, University of California, Berkeley
2121 Etcheverry Hall
Berkeley, CA 94720
No conflicts of interest

1 Abstract

2
3 Carbon-fiber reinforced (CFR) PEEK implants are used in orthopedic applications ranging from
4 fracture fixation plates to spinal fusion cages. Documented implant failures and increasing
5 volume and variety of CFR PEEK implants warrant a clearer understanding of material behavior
6 under monotonic and cyclic loading. To address this issue, we conducted monotonic and fatigue
7 crack propagation (FCP) experiments on orthopedic grade unfilled PEEK and two formulations
8 of CFR PEEK (PAN- and pitch-based carbon fibers). The effect of annealing on FCP behavior
9 was also studied. Under monotonic loading, fiber type had a statistically significant effect on
10 elastic modulus (12.5 ± 1.3 versus 18.5 ± 2.3 GPa, pitch versus PAN CFR PEEK, $AVG \pm SD$)
11 and on ultimate tensile strength (145 ± 9 versus 192 ± 17 MPa, pitch versus PAN CFR PEEK,
12 $AVG \pm SD$). Fiber type did not have a significant effect on failure strain. Under cyclic loading,
13 PAN CFR PEEK demonstrated an increased resistance to FCP compared with unfilled and pitch
14 CFR PEEK, and this improvement was enhanced following annealing. Pitch CFR PEEK
15 exhibited similar FCP behavior to unfilled PEEK and neither material was substantially affected
16 by annealing. The improvements in monotonic and FCP behavior of PAN CFR PEEK is
17 attributed to a compound effect of inherent fiber properties, increased fiber number for an
18 equivalent wt % reinforcement, and fiber aspect ratio. FCP was shown to proceed via cyclic
19 modes during stable crack growth, which transitioned to static modes (more akin to monotonic
20 fracture) at longer crack lengths. The mechanisms of fatigue crack propagation appear similar
21 between carbon-fiber types.

22 1. Introduction

23 Poly(ether-ether-ketone) (PEEK) is a high-performance, biocompatible polymer which
24 has been used in load-bearing orthopedic components since the 1990s [1]. The ability to
25 formulate PEEK with fillers such as carbon fiber can result in mechanical properties suitable to a
26 variety of orthopedic applications, including spinal fusion cages, fracture fixation plates, femoral
27 stems, bone screws, intramedullary nails, and other devices [2].

28 The mechanical and thermal properties of PEEK are a function of its crystalline structure,
29 chemical architecture, and morphology. PEEK is a semi-crystalline thermoplastic which,
30 depending on processing, can be up to 43% crystalline [3], although 30-35% crystallinity
31 is typical for PEEK used in medical devices [1,4,5]. The crystalline domains are generally
32 lamellar in structure and can organize into spherulites [3,6]. Crystallinity can be controlled by
33 altering the rate of cooling from the molten state during processing, or by using a post-processing
34 thermal treatment such as annealing. Since molecular chains need time and energy to organize
35 into crystalline domains, both slow cooling from the molten state and annealing enhance
36 crystallinity in PEEK. Fillers such as carbon fiber also affect morphology by altering the
37 geometry of crystalline domains as well as local cooling rates of the PEEK matrix [4,7-9].

38 The chemical backbone of PEEK is comprised of aromatic (benzene) units connected by
39 ketone and ether groups. The monomer units form a linear homopolymer with approximately
40 100 units per chain and an average molecular weight of 80,000-120,000 g/mol [1]. While the
41 molecule can rotate about the ether and ketone bonds, the large aromatic units inhibit chain
42 mobility and require large amounts of thermal energy for bulk motion [1,4]. Accordingly, PEEK
43 has a high glass transition temperature (145°C), a high melting temperature (340°C) [6] and is
44 stable at the body's operating temperature of 37°C.

45 In addition to its thermal and mechanical properties, PEEK's radiolucency and radiative
46 stability contribute to its orthopedic relevance. Metallic implants are radiopaque, inhibiting
47 radiographic assessment of intra-implant bone formation by causing artefacts that can hinder
48 clinical evaluation [10,11]. PEEK is radiolucent, enabling radiographic assessment using
49 existing diagnostic imaging techniques [2]. In the spine, for example, radiographic evidence of
50 bone density changes within a PEEK fusion cage can be used to assess the degree of fusion [12].
51 PEEK is stable when exposed to gamma radiation in doses relevant to implant sterilization (25-
52 40 kGy) [2], and can also be sterilized using steam and ethylene oxide without appreciable
53 degradation in mechanical properties [13].

54 The predominant clinical use of PEEK is in interbody fusion cages in the spine, where it
55 is used in approximately 65% of the spinal fusion devices implanted annually in the U.S. [14].
56 PEEK has also shown promise in fracture fixation plates [15,16] and femoral stems [17,18].
57 Stress shielding in metallic fracture fixation plates [19] and hip stems [20] has motivated
58 research into alternative structural materials, including PEEK. The use of carbon fiber to create
59 a reinforced PEEK composite enables the modulus of some PEEK formulations to approximate,
60 for example, cortical bone (approximately 17 GPa [21]), thereby theoretically reducing stress
61 shielding. A number of carbon-fiber-reinforced (CFR) PEEK fracture fixation devices are now
62 available and have shown promising clinical results [15,16]. PEEK as a femoral stem material
63 has been the subject of much research and promising medium-term clinical results [22] but
64 limited adoption in the U.S. While PEEK is used in only a fraction of the fracture fixation plates
65 and hip stems implanted annually, its use is expected to rise with continued research and longer-
66 term clinical data. This is especially relevant given the ongoing challenges with tissue modulus
67 matching in orthopedic metals and the propensity for corrosion in metallic devices.

68 Unfilled and CFR PEEK have also been explored as bearing surfaces for total joint
69 arthroplasty. *In vitro* tribological studies comparing the wear behavior of ultra-high-molecular-
70 weight polyethylene (UHMWPE) with unfilled and CFR PEEK have shown mixed results [23–
71 25]. Improvements in UHMWPE wear behavior, mixed PEEK data, and historical failures of
72 CFR polymer bearing surfaces dating back to the 1970s may limit PEEK’s use as a bearing
73 material in the near-term. Nonetheless, new PEEK formulations are being developed and
74 marketed as bearing surface alternatives [26].

75 CFR PEEK used in orthopedics commonly utilize one of two carbon-fiber types: PAN-
76 based carbon fibers or pitch-based carbon fibers. PAN-based carbon fibers are derived from
77 polyacrylonitrile and predominantly contain acrylonitrile monomer units, whereas pitch-based
78 carbon fibers are typically derived from petroleum products and contain thousands of aromatic
79 hydrocarbons [27,28]. The differences in carbon-fiber precursor requires different processing
80 conditions and results in different fiber geometric and mechanical properties [27]. PAN-based
81 carbon fibers can be stiffer, stronger, and are typically thinner than pitch-based carbon fibers
82 (fiber elastic modulus 540 versus 280 GPa, fiber diameter 6 - 8 versus 10 - 20 μm , PAN versus
83 pitch) [27,29,30]. The smaller diameter of PAN- compared to pitch-based carbon fibers as well
84 as fiber density differences can result in more numerous fibers within a PAN CFR PEEK
85 composite compared to a pitch CFR PEEK composite for an equivalent wt % reinforcement.
86 Accordingly, PAN CFR PEEK composites can be stiffer and stronger than pitch-based
87 counterparts [29]. Tribologically, PAN and pitch CFR PEEK exhibit similar wear rates, though
88 these rates are sensitive to ambient temperature [27], dry versus lubricated articulation [25],
89 conformity of contact [23], among other variables. Although tribological properties appear
90 largely similar, pitch CFR PEEK is marketed as a material with beneficial tribological properties

91 (tradename PEEK-OPTIMA Wear PerformanceTM) [26].

92 While not common, *in vivo* fractures of PEEK implants have been documented in the
93 literature [31,32]. Additionally, *in vivo* fractures of other orthopedic devices comprising
94 polymers (namely UHMWPE) and metals (namely cobalt-chromium, titanium, and stainless
95 steel), have been documented extensively [33–35] and remain a limiting factor in clinical
96 longevity. Despite the low prevalence of PEEK fractures, continually evolving material
97 formulations and component designs warrant an understanding of the monotonic and fatigue
98 fracture behavior of unfilled and pitch and PAN CFR PEEK.

99 A number of studies have explored effects of microstructural and processing variables on
100 the fatigue and fracture behavior of PEEK [36–44]. In both unfilled and reinforced PEEK,
101 matrix molecular weight can strongly influence fatigue crack propagation (FCP) resistance and
102 the mechanisms of crack propagation [36,37,42]. An increase in molecular weight has been
103 shown to improve resistance to FCP, an effect which has been partially attributed to an increased
104 density of tie molecules connecting lamellar regions in higher molecular weight formulations,
105 thereby strengthening the polymer matrix [36,37]. In unfilled PEEK, it has been shown that
106 matrix molecular weight can precipitate differences in spherulite size, whereby spherulites will
107 tend to grow larger in lower molecular weight PEEK [42]. Subsequently, crack growth tends to
108 be intraspherulitic in lower molecular weight PEEK (i.e. through larger spherulites) and
109 interspherulitic in higher molecular weight PEEK (i.e. around smaller spherulites) [42],
110 reflecting fundamentally different mechanisms of crack propagation as a function of molecular
111 weight. Enhanced crystallinity, which can be achieved via annealing [36,41,45], has also been
112 shown to enhance resistance to FCP, though to a much lesser extent than molecular weight
113 [36,37]. The mechanisms driving this improvement in FCP resistance are attributed to increased

114 energy required to deform and crack organized crystalline domains compared with amorphous
115 domains [36,37]. Interestingly, while annealing increases the degree of crystallinity in unfilled
116 and reinforced PEEK by similar amounts, improvements in FCP resistance induced by annealing
117 have been shown to be greater in reinforced PEEK compared with unfilled PEEK [36]. It has
118 been suggested that strong carbon fiber/PEEK matrix bonding produces crack initiation close to
119 but not at the fiber/matrix interface (small amounts of matrix material may remain attached to the
120 fibers), and thus FCP in short CFR PEEK is strongly dependent or even dominated by matrix
121 properties, such as crystallinity, in regions close to the fibers [36]. The importance of the matrix
122 properties in FCP in short CFR PEEK is supported by saturating improvements in FCP resistance
123 with increasing fiber volume fraction [44]. While the addition of carbon fibers to a PEEK matrix
124 introduces new energy dissipation mechanisms via fiber fracture and pullout, it also constrains
125 the ability of the matrix to dissipate energy via plastic deformation [44]. Fiber fractions of 30%
126 wt appear to offer little improvement in FCP resistance compared to volume fractions of 20% wt
127 due to these competing energy dissipation mechanisms [44], thus underscoring the importance of
128 matrix plasticity in FCP.

129 While previous studies have elucidated some microstructural and processing variables on
130 the fatigue and fracture behavior of PEEK, there have been no studies directly comparing the
131 FCP behavior of PAN versus pitch CFR PEEK. In light of documented *in vivo* fractures of
132 orthopedic implants made of both polymeric and metallic components coupled with PAN and
133 pitch CFR PEEK formulations designed specifically for orthopedic applications, it is the aim of
134 the present investigation to describe the monotonic and FCP behavior of unfilled PEEK and pitch
135 and PAN CFR PEEK. Additionally, the effect of annealing on FCP behavior is investigated.
136 The materials studied were formulated specifically for use in orthopedic implants.

137 2. Methods

138 2.1 Material formulations

139 Three PEEK material formulations were studied:

140 (1) Unfilled PEEK (density 1.3 g/cm³, tradename PEEK-OPTIMA™ LT1, Invibio,
141 Lankashire, UK)

142 (2) PAN CFR PEEK (density 1.3 g/cm³, PEEK-OPTIMA™ LT1 matrix with 30% wt
143 PAN carbon fibers, tradename PEEK-OPTIMA Reinforced™, Invibio, Lankashire, UK).
144 Fibers are short and randomly distributed (fiber modulus 540 GPa, fiber diameter 6 ± 2
145 μm, fiber length 230 ± 23 μm, fiber density 1.8 g/cm³ [45])

146 (3) Pitch CFR PEEK (density 1.4 g/cm³, PEEK-OPTIMA™ LT1 matrix with 30% wt
147 Pitch carbon fibers, tradename PEEK-OPTIMA Wear Performance™, Invibio,
148 Lankashire, UK). Fibers are short and randomly distributed (fiber modulus 280 GPa,
149 fiber diameter 10 ± 2 μm, fiber length 230 ± 13 μm, fiber density 2.0 g/cm³ [45])

150 Material granules were obtained from Invibio and processed into dog-bone and compact-
151 tension (CT) specimens (Figure 1). Granules were first pre-heated to 70°C to remove residual
152 moisture then injection molded into plates (250 x 25 x 2.5 mm). The injection nozzle
153 temperature was held constant at 400°C and the mold at 250°C. Samples were cooled in air at
154 room temperature. Water-jet machining was used to cut dog-bone and CT specimens from the
155 plates, with the samples oriented for load application parallel to the mold-fill direction.

156 Three heat treatments were examined to investigate the effects of post-processing thermal
157 treatment on FCP behavior. Samples were either non-annealed, annealed at 200°C, or annealed
158 at 300°C. Annealing was conducted for five hours in a Nabertherm oven (Lilienthal, Germany),

159 with an initial heating rate of 5°C/min. After annealing, samples were cooled in air at room
160 temperature. Annealing was performed by Lima Corporate (Udine, Italy).

161 **2.2 Monotonic testing**

162 Tensile testing to failure was performed on non-heat-treated samples in accordance with
163 ASTM D638 on type V dog-bone specimens (n=4 samples tested per material for a total of 12
164 tests). Monotonic mechanical testing for equivalent heat-treated materials has been reported
165 elsewhere [25,46] and was therefore not repeated here. Displacement was applied at a rate of 0.5
166 mm/min in ambient conditions (21°C / 28% RH) using a screw-driven Instron (model 5500R).
167 Strain was measured using a video extensometer (Instron, model 2663-821). Temperature of the
168 gauge-section was not measured during monotonic testing. Due the viscoelastic nature of
169 thermoplastic polymers, reported mechanical properties should be understood within the context
170 of displacement rate and ambient temperature. However, it has been previously shown that at
171 room temperature (≈ 124 °C below PEEK's glass transition temperature), varying displacement
172 rate by over four orders of magnitude (from 0.05 to 50 mm/min) had little effect on elastic
173 modulus and increased yield stress by less than 1.4x [47].

174 Elastic modulus (E), ultimate tensile strength (σ_{ut}), and elongation at failure (ϵ_f) were
175 reported for each material. Elastic modulus was calculated using a secant approximation
176 between 0.1% and 0.5% strain for each specimen. Student's t-tests were used to compare E, σ_{ut} ,
177 and ϵ_f between material formulations with significance assumed at $p \leq 0.05$.

178 **2.3 Fatigue testing**

179 Fatigue crack propagation (FCP) experiments were conducted on CT specimens using a
180 servo-hydraulic Instron (model 8871) and a load-controlled sinusoidal wave function at a
181 frequency of 5 Hz [41,43]. Testing was performed at room-temperature and an air-cooling

182 system was used to minimize hysteretic heating [48]. The load ratio (minimum load/maximum
 183 load) was held constant at 0.1. A pre-crack of 1 mm was introduced at the tip of each notch
 184 using a razor blade and custom fixture, and datum dots were placed on specimen sides for
 185 subsequent image analysis [48]. Crack length was measured using a variable magnification
 186 optical system (Infinivar CFM-2/S, 5 μ m/pixel) and a digital video camera (Sony XCD-SX910).
 187 A custom LabView program controlled the camera, which captured images every 500 or 1000
 188 cycles, depending on crack velocity. Custom scripts were created in ImageJ and MATLAB to
 189 semi-automate data analysis. A minimum of three samples were tested for each material
 190 formulation. The Paris equation (Equation 1) was used to map FCP as a function of cyclic stress
 191 intensity, where da/dN is the rate of crack velocity (mm/cycle), ΔK is the cyclic stress intensity
 192 (i.e. the crack driving force, MPa \sqrt{m}), and C (pre-exponent) and m (exponent, slope on
 193 logarithmic scale) are material constants. Any data not meeting the condition of small scale
 194 yielding (Equation 2) were excluded from this analysis, where (W-a) is the uncracked ligament
 195 length, K_{max} is the maximum mode-one stress intensity (MPa \sqrt{m}), and σ_{ys} is the material yield
 196 strength (MPa).

$$197 \quad \left. \begin{array}{l} \frac{da}{dN} = C\Delta K^m \end{array} \right\} \text{Equation 1}$$

$$198 \quad (W - a) \geq \frac{4}{\pi} \left(\frac{K_{max}}{\sigma_{ys}} \right)^2 \quad \text{Equation 2}$$

199 **2.4 Fractography**

200 Fracture surfaces were imaged with scanning electron microscopy (SEM, Quanta FEI and
 201 Versa 3D Dual Beam) at 50-500x and optical microscopy (Keyence VHX 6000) at 10-50x.
 202 Some specimens were sputter coated in gold-vanadium to facilitate fracture surface visualization.

203 **3. Results**

204 **3.1 Monotonic testing results**

205 Compared with pitch CFR PEEK, PAN CFR PEEK exhibited a significantly higher
206 elastic modulus (18.5 ± 1.3 vs 12.5 ± 1.3 GPa, PAN vs pitch CFR PEEK, $p = 0.006$, AVG \pm SD)
207 and ultimate tensile strength (192 ± 17 vs 145 ± 9 MPa, PAN vs pitch CFR PEEK, $p = 0.005$,
208 AVG \pm SD) (Table 1). Strain at failure was not significantly different between fiber types ($1.9 \pm$
209 0.2 vs 2.2 ± 0.2 % strain, PAN vs pitch CFR PEEK, $p = 0.116$, AVG \pm SD) (Table 1). Unfilled
210 PEEK had a significantly lower elastic modulus (3.9 ± 0.2 GPa, AVG \pm SD) and ultimate tensile
211 strength (93 ± 1 MPa), and a significantly higher strain at failure (66 ± 7 %, AVG \pm SD)
212 compared with either fiber type ($p \leq 0.002$) (Table 1). In terms of the stress-strain behavior,
213 unfilled PEEK demonstrated appreciable post-yield deformation (necking), whereas both pitch
214 and PAN CFR PEEK failed in a predominantly brittle manner, at low failure strains and with
215 little post-yield deformation (Figure 2).

216 **3.2 Fatigue testing results**

217 The crack velocity (da/dN) versus cyclic stress intensity (ΔK) curves for all PEEK
218 materials generally followed a linear relationship in log-log space as described by the Paris Law
219 (Equation 1, Figure 3). The region of stable crack growth was measured as $3.2 \leq \Delta K \leq 7.1$
220 $\text{MPa}\sqrt{\text{m}}$ for unfilled PEEK, $4.2 \leq \Delta K \leq 6.8$ $\text{MPa}\sqrt{\text{m}}$ for pitch CFR PEEK, and $4.6 \leq \Delta K \leq 8.6$
221 $\text{MPa}\sqrt{\text{m}}$ for PAN CFR PEEK (all heat treatments). A rightward shift was observed in the PAN
222 CFR PEEK data compared with the pitch CFR and unfilled PEEK data (all heat treatments).
223 This rightward shift suggests an improvement in FCP resistance—a larger cyclic stress intensity
224 was required to propagate a crack at a given velocity. The effect of annealing on FCP behavior
225 appears small for unfilled and pitch CFR PEEK, evidenced by largely overlapping da/dN versus
226 ΔK data (Figure 3). Annealing at 300 °C appears to have a more pronounced effect for PAN

227 CFR PEEK, evidenced by the distinct da/dN versus ΔK data between PAN and PAN 300 (Figure
228 3).

229 To clarify and quantify these observations, least squares regression analysis was used to
230 generate best fit lines of the data (Figure 4). ΔK values at a constant crack velocity of $da/dN = 2$
231 $\times 10^{-4}$ mm/cycle were compared in order to quantify the relative resistance to FCP as well as the
232 effect of annealing at an intermediate crack velocity (Table 2). The value of $da/dN = 2 \times 10^{-4}$
233 mm/cycle was chosen because it represents a crack velocity approximately centered within the
234 linear (Paris) growth regime, approximately halfway between near-threshold and near fast-
235 fracture regions based on the spread of the measured data (Figure 3, Figure 4). For non-annealed
236 formulations, propagating a crack at $da/dN = 2 \times 10^{-4}$ mm/cycle required $\Delta K = 4.9$ MPa \sqrt{m} for
237 unfilled PEEK, $\Delta K = 4.7$ MPa \sqrt{m} for pitch CFR PEEK, and $\Delta K = 5.7$ MPa \sqrt{m} for PAN CFR
238 PEEK (Table 2). Thus, non-annealed unfilled and pitch CFR PEEK require a similar ΔK for
239 intermediate crack velocities while non-annealed PAN CFR PEEK requires an increased ΔK on
240 the order of 17-21% compared with unfilled and pitch CFR PEEK, respectively. For
241 formulations annealed at 300 °C, the ΔK values required to propagate a crack at $da/dN = 2 \times 10^{-4}$
242 mm/cycle remain similar between unfilled and pitch CFR PEEK (4.7 versus 4.8 MPa \sqrt{m} ,
243 respectively) but increased to 7.0 MPa \sqrt{m} for PAN CFR PEEK, representing an increase of 45-
244 50%.

245 The effect of heat-treatment on FCP resistance was thus relatively minor for unfilled
246 PEEK, with a maximum ΔK variation of 0.3 MPa \sqrt{m} (6%) amongst heat treatments at $da/dN = 2$
247 $\times 10^{-4}$ mm/cycle. Similarly, the effect of heat treatment was relatively minor for pitch CFR
248 PEEK, with a maximum ΔK variation of 0.5 MPa \sqrt{m} (9%) amongst heat treatments at $da/dN = 2$
249 $\times 10^{-4}$ mm/cycle. Conversely, heat-treatment had a larger effect on PAN CFR PEEK, with a

250 maximum ΔK variation of 1.5 MPa \sqrt{m} (24%) amongst heat treatments at $da/dN = 2 \times 10^{-4}$
251 mm/cycle.

252 The linear regression analysis also enabled calculation of the Paris exponent (m in
253 Equation 1), a material-specific parameter describing the rate of crack acceleration. Larger
254 values of m indicate larger rates of crack accelerations. Values of m ranged between 4 - 5.1 for
255 unfilled PEEK, 6.6 – 8.0 for pitch CFR PEEK, and 5.9 – 6.3 for PAN CFR PEEK (Figure 5).
256 Thus, we observe a trend towards larger values of crack acceleration for both pitch and PAN
257 CFR PEEK compared with unfilled PEEK, suggesting that the addition of carbon-fibers can
258 increase the rate of crack acceleration. Heat-treatment appeared to have a minor and non-
259 constant effect on m (Figure 5). In unfilled and pitch CFR PEEK, annealing decreased m ,
260 whereas for PAN CFR PEEK, annealing at 200 °C and 300 °C resulted in an increase in m of
261 17% and 7%, respectively (6.9 and 6.3 versus 5.9).

262 **3.3 Fractography**

263 Under monotonic loading, the fracture surface of unfilled PEEK displayed macroscopic
264 plastic deformation including tearing features and a reduced cross-sectional area at the location
265 of fracture (a result of necking) (Figure 6). The fracture surfaces of pitch and PAN CFR PEEK
266 were similar to each other, displaying little bulk plastic deformation in comparison with unfilled
267 PEEK (Figure 6). Pitch and PAN CFR PEEK display fiber fracture and fiber pull-out throughout
268 the fracture surface (Figure 6).

269 Under fatigue loading, unfilled PEEK exhibited striation-like markings and parabolic
270 features in the stable growth regime (Figure 7). The parabolic features tended to grow larger at
271 longer crack lengths (Figure 7E). Compared with the stable growth region, the unstable growth

272 region in unfilled PEEK exhibited much greater amounts of plastic deformation, evidenced by
273 localized contraction (necking) around the crack tip (Figure 7A).

274 Pitch and PAN CFR PEEK present with little macroscopic deformation (Figure 8),
275 resulting from suppression of plastic deformation due to the presence of carbon fibers. During
276 stable FCP, some fiber fracture and pull-out were observed in combination with near-tip local
277 deformation of the matrix material (Figure 8B, 8E). During unstable FCP, these local matrix
278 deformation features are not observed and the fracture surfaces instead display primarily fiber
279 fracture and fiber pull-out (Figure 8C, 8F).

280 There were no observable fractographic distinctions in macroscopic (reinforcement-level)
281 failure mode or mechanism between heat-treatments for unfilled PEEK and pitch and PAN CFR
282 PEEK. Higher imaging magnifications may illuminate crystalline-level mechanisms and
283 warrants further investigation.

284 **4. Discussion**

285 It was the aim of the current study was to investigate the effects of PAN- and pitch-based
286 carbon fibers on the monotonic properties and FCP resistance of orthopedic grade PEEK.
287 Additionally, we sought to elucidate the effects of annealing on FCP resistance.

288 Complete crystallinity data for the materials used in this study have been reported
289 elsewhere [25]. Briefly, crystallinity for non-annealed PEEK is $\approx 32\%$, and all non-annealed
290 formulations (i.e. unfilled, pitch and PAN CFR PEEK) are within 1% of this value [25].
291 Annealing enhances crystallinity in unfilled and pitch and PAN CFR PEEK by similar amounts:
292 Low temperature (200 °C) annealing enhances crystallinity by $\approx 1\%$ while high temperature (300
293 °C) annealing enhances crystallinity by $\approx 9\%$ [25].

294 The addition of both pitch and PAN carbon fibers to the PEEK matrix increased
295 monotonic stiffness and strength and decreased ductility (strain to failure) compared with
296 unfilled PEEK. These trends are consistent with data published by the material manufacturer
297 [26,49,50] and with the behavior of many short-fiber thermoplastic polymer composites.
298 Comparing fiber types, we observed statistically significant increases of 48% in elastic modulus
299 and 32% in ultimate tensile strength, and a non-statistically significant decrease of 14% in strain
300 to failure for PAN versus pitch CFR PEEK. Increases in elastic modulus and ultimate tensile are
301 attributed to a number of microstructural characteristics, including inherent fiber mechanical
302 properties, differences in fiber number, and differences in fiber aspect ratio. The PAN-based
303 carbon fibers used in this study are 93% stiffer than pitch-based carbon fibers (elastic modulus
304 540 versus 280 GPa, PAN- versus pitch-based carbon fibers, respectively) [29]. Thus, composite
305 mechanical property differences would be expected even if other parameters (fiber number, fiber
306 aspect ratio, interfacial bonding, crystallinity, etc.) were equivalent. Further, PAN-based carbon
307 fibers are thinner and less dense than pitch-based carbon fibers (diameter 6 versus 10 μm ,
308 density 1.8 versus 2.0 g/cm^3 , PAN- versus pitch-based carbon fibers, respectively), and we thus
309 expect ≈ 3.1 times more PAN-based carbon fibers in a given specimen compared with pitch-
310 based carbon fibers for an equivalent wt % reinforcement (both composites used in this study
311 contained 30% wt fiber reinforcement). In a related vein, since the diameter of PAN-based
312 carbon fibers are smaller than pitch-based carbon fibers, the ratio of fiber surface area to fiber
313 volume will be enhanced in PAN versus pitch CFR PEEK for an equivalent fiber volume
314 fraction, thereby providing more surface area for the PEEK matrix to bond to PAN-based carbon
315 fibers. We suggest that improvements in mechanical behavior for PAN versus pitch CFR PEEK
316 are attributed to these compound effects: PAN-based carbon fibers are themselves stiffer, more

317 PAN-based carbon fibers are present, and comparatively more PAN-based carbon fiber surface
318 area is exposed to PEEK matrix, thus enhancing the area available for fiber/matrix bonding.

319 Under fatigue loading, we found that the addition of pitch-based carbon fibers did not
320 enhance FCP resistance, as the da/dN versus ΔK behavior for unfilled and pitch CFR PEEK are
321 similar. FCP resistance of these materials was largely unaffected by either low-temperature (200
322 °C) or high-temperature (300 °C) annealing. Conversely, the FCP resistance of PAN CFR PEEK
323 was appreciably improved compared with unfilled and pitch CFR PEEK. For non and low-
324 temperature annealed PAN CFR PEEK, the improvement was on the order of 17-21%, while for
325 high-temperature annealed PAN CFR PEEK the improvement was on the order of 45-50% at an
326 intermediate crack velocity.

327 The complex interdependence of microstructural parameters including manufacturing-
328 and annealing-induced matrix crystallinity, fiber type, fiber number, and fiber aspect ratio,
329 coupled with complex dynamics of FCP in polymer composites, make it difficult to
330 unambiguously differentiate individual microstructural effects on FCP behavior. Yet, a number
331 of observations warrant discussion.

332 The addition of fibers to a polymer matrix can enhance resistance to FCP by introducing
333 energy dissipation mechanisms via fiber fracture and pull-out [44]. Simultaneously, fibers can
334 inhibit energy dissipation by limiting the ability of the matrix to deform plastically [44]. The
335 balance between net energy dissipation/absorption (thus FCP improvement/degradation) depends
336 on a balance between matrix ductility (which depends on matrix molecular weight, crystallinity,
337 etc.), fiber properties, and the properties of the fiber/matrix interface. Previous studies have
338 shown that the addition of 30% wt. randomly distributed short glass fibers to a PEEK matrix
339 provided little to no improvement in FCP resistance, while the addition of 30% wt. randomly

340 distributed carbon fibers provided at least some improvement in FCP resistance [36,41,43] (the
341 carbon fiber type is not mentioned in these studies, however PAN-based carbon fibers are the
342 likely historical precedent [51]). This phenomenon is attributed to stronger fiber/matrix adhesion
343 between the carbon fibers and the PEEK matrix compared with glass fibers and the PEEK matrix
344 [36,41,44]. The results found in the current study, in which the addition of pitch-based carbon
345 fibers provided little to no improvement in FCP resistance, while the addition of PAN-based
346 carbon fibers provided an appreciable improvement in FCP resistance, could be plausibly
347 explained via the same mechanism; stronger fiber/matrix adhesion in PAN- compared with pitch-
348 based PEEK composites. However, aforementioned differences in inherent fiber properties, fiber
349 numbers, and fiber aspect ratios confound and preclude a definitive statement on interfacial bond
350 strength. Indeed, the fact that observed improvements in FCP resistance for PAN CFR PEEK
351 are not commensurate with the magnitude of differences in fiber properties or fiber number could
352 plausibly suggest a weaker interfacial bond for PAN versus pitch CFR PEEK. Additional studies
353 are required to clarify differences in interfacial bond strength, which could be achieved via FCP
354 tests controlling for fiber aspect ratio and/or fiber number.

355 Annealing has been shown to have a greater impact on FCP resistance for CFR PEEK
356 compared with unfilled PEEK (carbon fiber type not specified), even when similar overall
357 increases in crystallinity are induced by annealing [36,41]. Results found in the current study for
358 PAN CFR PEEK are similar—annealing had no measurable effect on unfilled PEEK but
359 appreciably improved FCP resistance in PAN CFR PEEK. It has been suggested that annealing
360 may preferentially influence the matrix in regions near the fiber/matrix interface [36]. Thus,
361 while it is not clear why annealing had no measurable effect on pitch CFR PEEK, one plausible
362 explanation is that a lower fiber number in pitch versus PAN CFR PEEK (thus fewer

363 fiber/matrix interfacial regions) makes any preferential improvements in crystallinity less
364 pronounced. It has also been suggested that annealing enhances crystalline growth of the PEEK
365 matrix onto the carbon fiber surface, thereby improving interfacial bond strength [41]. Thus, a
366 second and related explanation follows that differences in crystallization mechanisms between
367 PAN and pitch CFR PEEK [45] contribute to differences in interfacial bond strength as a
368 function of annealing, even for similar overall degrees of crystallinity.

369 Fractographic analysis of failure surfaces suggest two distinct modes of FCP in PEEK,
370 notably a cyclic mode acting at low crack growth rates and a static mode acting at high crack
371 growth rates, as described by previous studies [37,38,40,43,44].

372 In unfilled PEEK, the stable growth regime exhibited striation-like markings (Figure 7B,
373 7C), similar to those reported previously [37,38,40,41,44], presumably caused by crack blunting
374 and re-sharpening during cyclic loading. The average width of the striation-like bands were not
375 measured in this study and compared to da/dN to confirm whether they were true fatigue
376 striations. Yet, previous investigations [37,40,41] confirmed markings of similar size and
377 morphology to be true fatigue striations. The observed parabolic features (Figure 7C, 7E) are
378 also consistent with previous investigations [37,41,44], and are attributed to the intersection of
379 the primary crack front with secondary cracks induced by inherent flaws. Unlike the stable
380 growth regime, the fast-fracture regime in unfilled PEEK is characterized by ductile contraction
381 (i.e. necking) in the zone around the crack tip. This ductile contraction in fast fracture region is
382 not apparent during stable crack growth but is apparent for monotonically tested PEEK.

383 Failure surfaces of pitch and PAN CFR PEEK also show evidence of an interaction
384 between cyclic and static mechanisms during FCP in line with previous studies on CFR PEEK
385 [44]. At low crack growth rates, we observe regions of matrix deformation and rupture near to

386 and along the fiber/matrix interface, as well as fiber fracture and pull-out (Figure 8B, 8E). It has
387 been previously shown that under cyclic loading, local failure is dominated by separation along
388 the fiber/matrix interfaces and rupture of the matrix material between fibers [36,43]. At higher
389 crack growth rates, equivalent matrix deformation is not observed, and the fracture surface is
390 instead comprised primarily of fiber fracture and pull-out (Figure 8C, 8F) more akin to
391 monotonically tested samples (Figure 6). Thus, our findings offer supporting evidence for cyclic
392 modes of growth at low growth rates which transition to static modes near the onset of failure in
393 unfilled and both pitch and PAN CFR PEEK.

394 While the CFR PEEK formulations used in this study were reinforced using short,
395 randomly distributed fibers to achieve bulk isotropy, the injection molding process has been
396 shown to introduce some fiber alignment in proximity to the specimen surface (i.e. a “skin”
397 layer) induced by friction with the mold wall [29,36,41,43,44]. This well-documented skin-core
398 structure has been shown to produce more rapid crack growth when load is applied perpendicular
399 to the mold-fill direction (thus crack growth parallel to the mold-fill direction) compared with the
400 converse orientation [43,44]. Thus, the results here are limited to load application parallel to the
401 mold fill direction.

402 **5. Conclusion**

403 Under monotonic loading, PAN CFR PEEK exhibited a larger elastic modulus and
404 ultimate tensile strength compared with unfilled and pitch CFR PEEK. Under cyclic loading,
405 PAN CFR PEEK exhibited an improved resistance to fatigue crack propagation compared with
406 unfilled and pitch CFR PEEK. The improvement in fatigue crack propagation resistance for
407 PAN CFR PEEK was enhanced following high-temperature (300 °C) annealing.

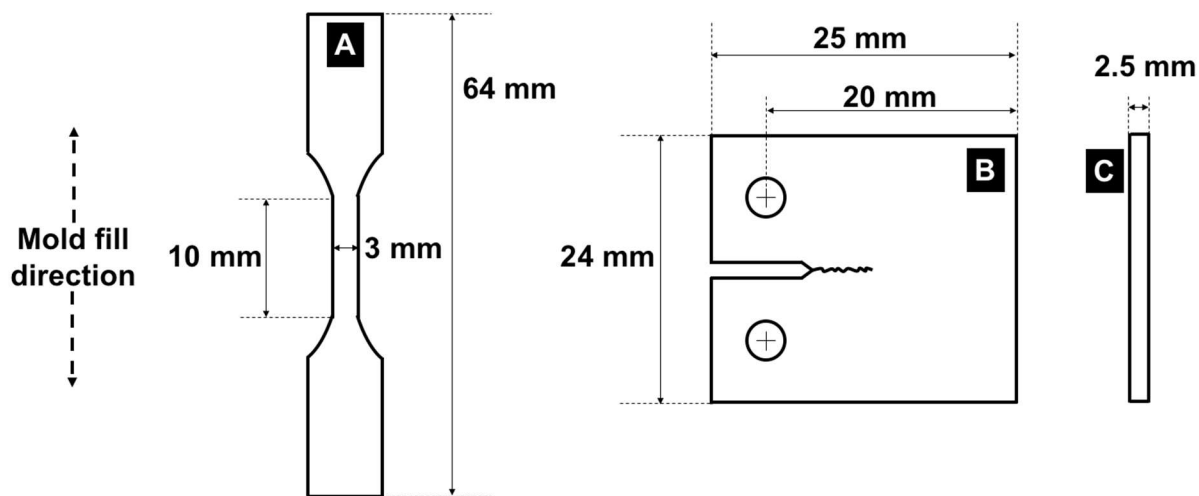
408 Pitch CFR PEEK did not exhibit improved fatigue crack propagation resistance compared
409 with unfilled PEEK. Neither low temperature (200 °C) nor high temperature (300 °C) annealing
410 produced a measurable effect on the fatigue crack propagation behavior of these materials.

411 The improvement in mechanical properties for PAN CFR PEEK is attributed to a
412 compound affect: PAN-based carbon fibers are themselves stiffer than pitch-based carbon fibers,
413 more PAN-based carbon fibers are present compared with pitch-based carbon fibers for an
414 equivalent wt % reinforcement, and comparatively more PAN-based carbon fiber surface area is
415 exposed to PEEK matrix, thus enhancing the area available for fiber/matrix bonding.
416 Differences in fiber/matrix interfacial bond strength between PAN- versus pitch-based carbon
417 fibers should be further elucidated, possibly via studies controlling for fiber number and/or
418 aspect ratio.

419 Fatigue crack propagation was shown to proceed via cyclic modes during stable crack
420 growth, characterized by striation-like bands and parabolic features in unfilled PEEK and matrix
421 rupture near to and along the fiber/matrix interface in pitch and PAN CFR PEEK. Cyclic modes
422 transition to static modes (more akin to monotonic fracture) at longer crack lengths,
423 characterized by necking in unfilled PEEK and an increased degree of fiber fracture and pull-out
424 in pitch and PAN CFR PEEK. The mechanisms of fatigue crack propagation appear similar
425 between carbon-fiber types.

426

427 6. Figures and Tables



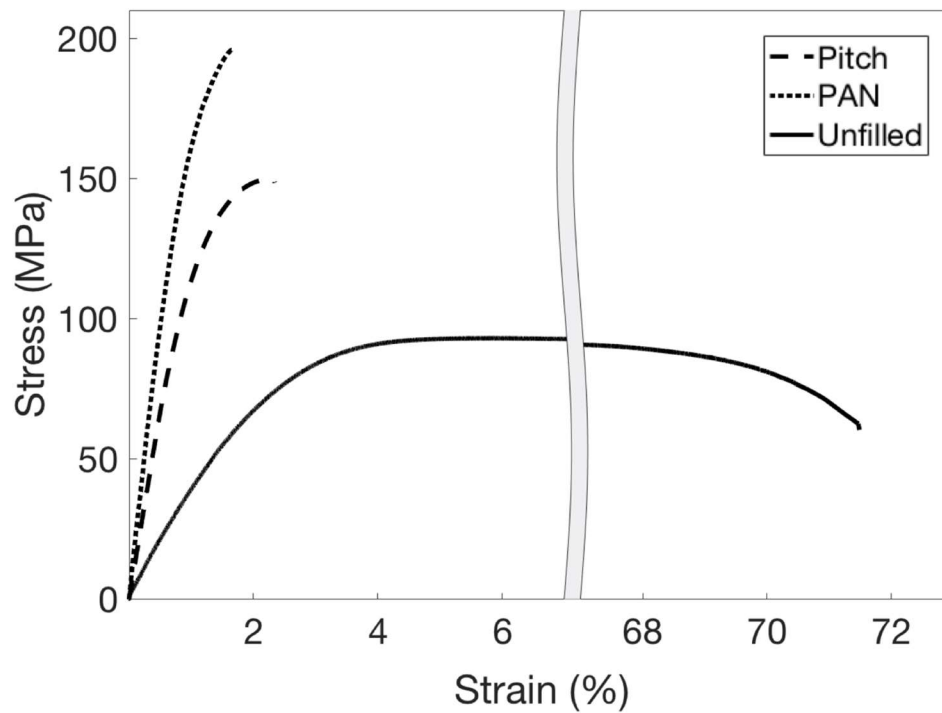
428
 429 Figure 1. A) ASTM D638 type V dog-bone specimens used for monotonic testing. B) Compact-
 430 tension (CT) specimen used for FCP testing. C) Thickness for all specimens. Samples were
 431 oriented for load application parallel to the mold fill direction. Drawings are not to scale.

432
 433
 434
 435
 436

Table 1. Material properties for PEEK materials (non-heat-treated formulations).

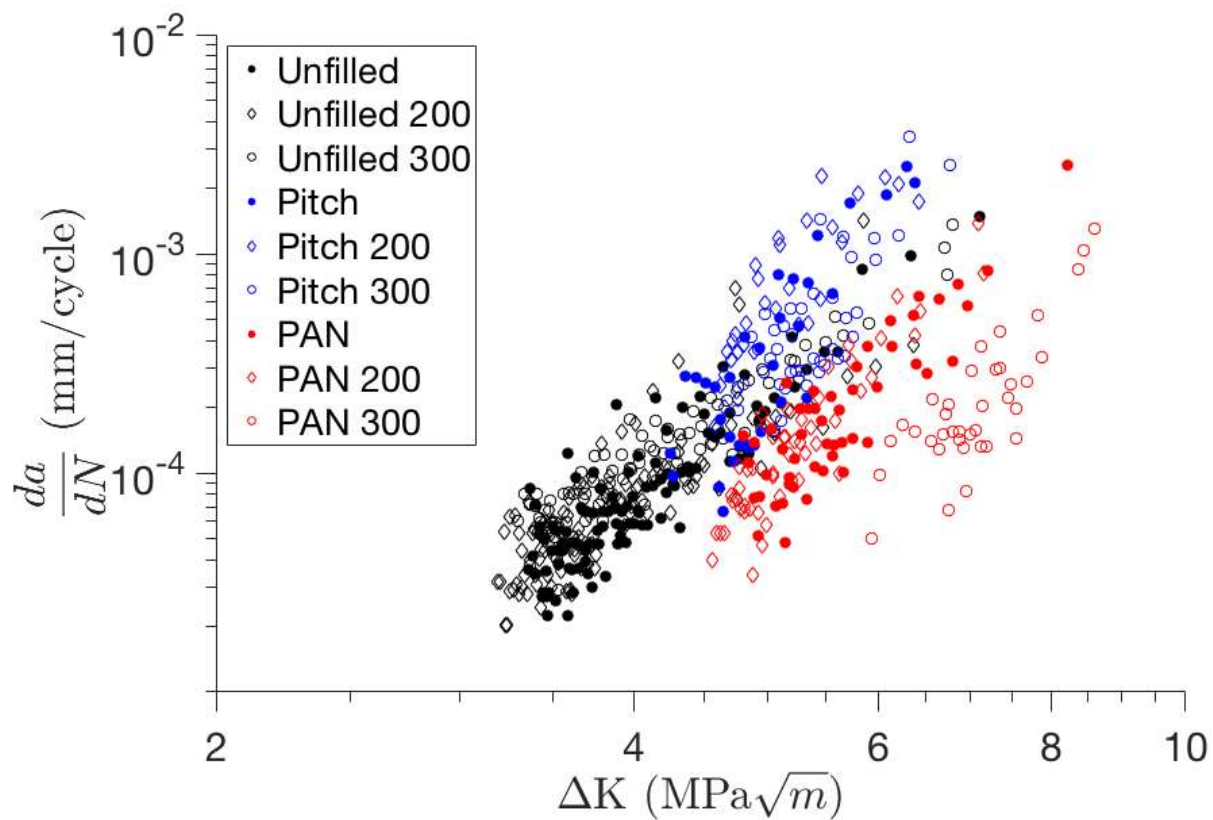
	Unfilled	Pitch	PAN
E (GPa)	3.9 ± 0.2	12.5 ± 1.3	18.5 ± 2.3
σ_{ut} (MPa)	93 ± 1	145 ± 9	192 ± 17
ϵ_f (%)	66 ± 7	2.2 ± 0.2	1.9 ± 0.2

437



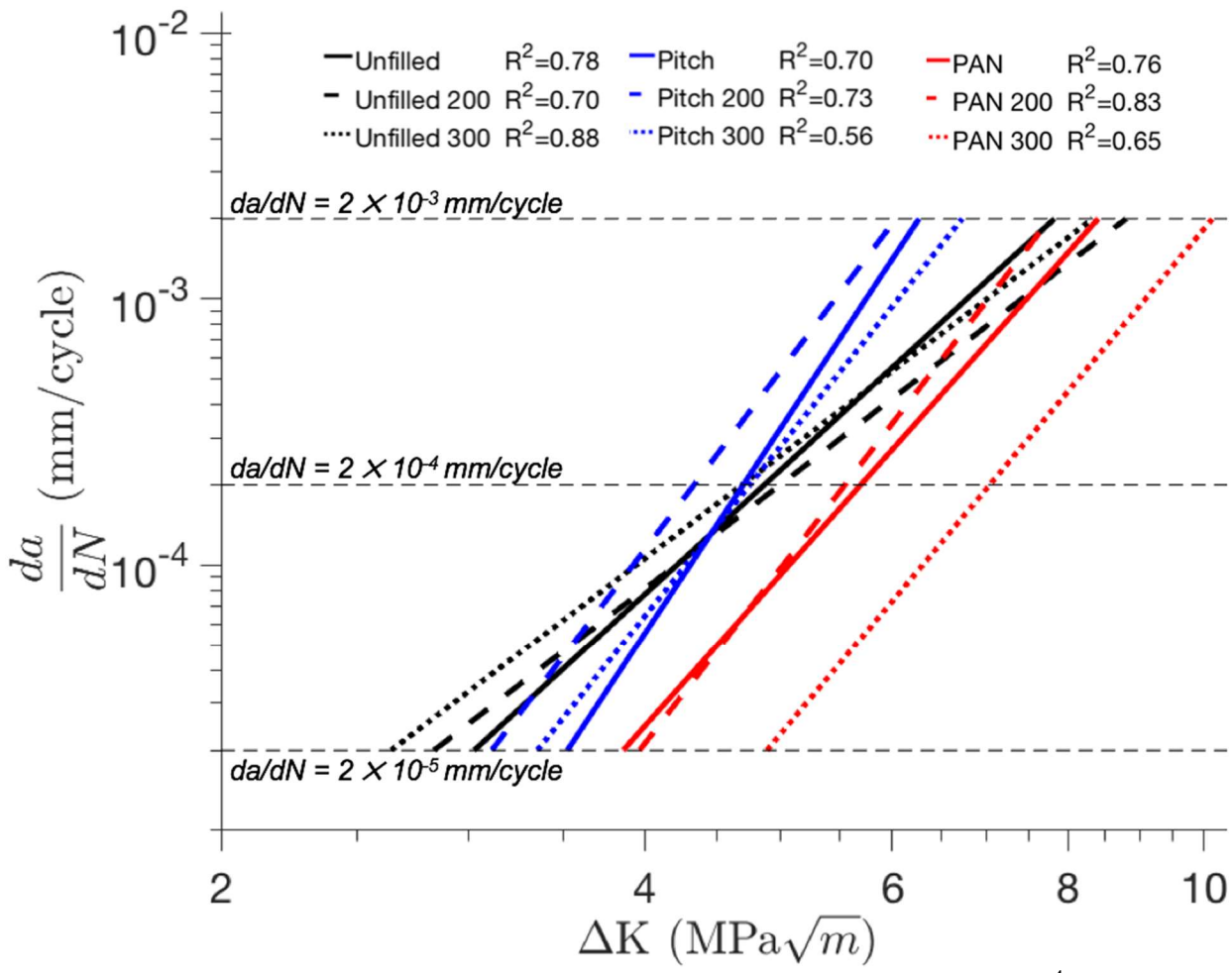
438
439
440
441
442
443

Figure 2. Representative stress-strain plots for Pitch CFR PEEK, PAN CFR PEEK, and unfilled PEEK (non heat-treated formulations).



444

445 Figure 3. FCP plots for all material formulations and heat-treatments.



446
447
448
449
450
451
452
453
454
455
456
457
458
459
460
461
462
463
464
465
466

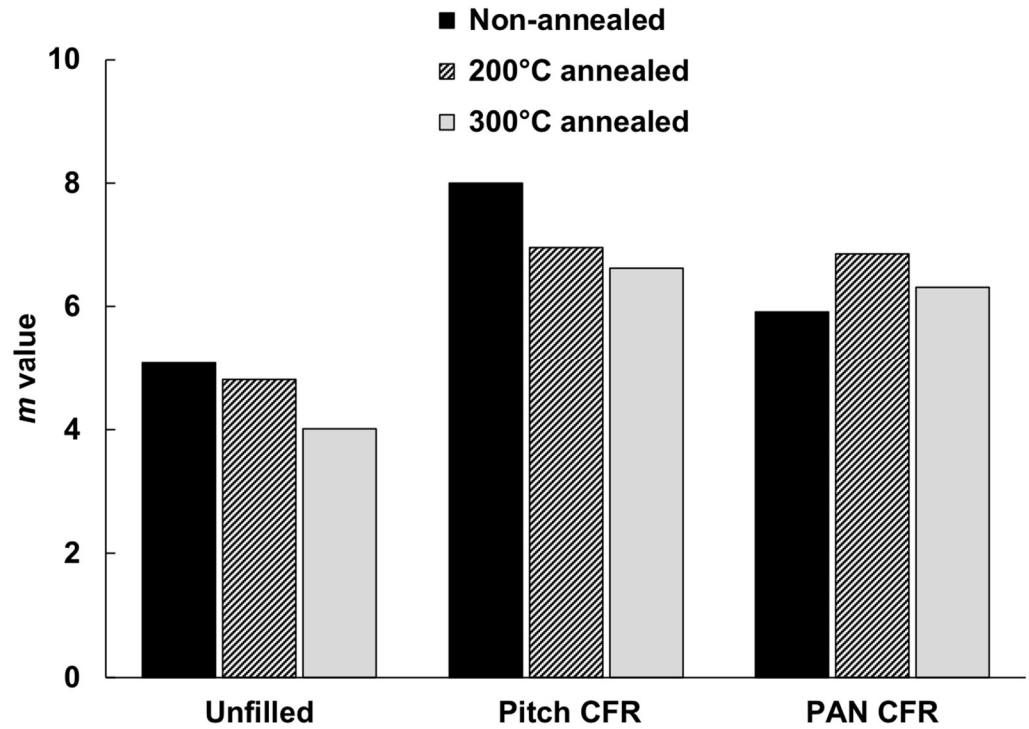
Figure 4. Paris fits for all materials. A constant crack velocity of $da/dN = 2 \times 10^{-4}$ mm/cycle was chosen to represent an intermediate crack velocity.

467
468
469

Table 2. ΔK values at the intermediate crack velocity of $da/dN = 2 \times 10^{-4}$ mm/cycle for all materials.

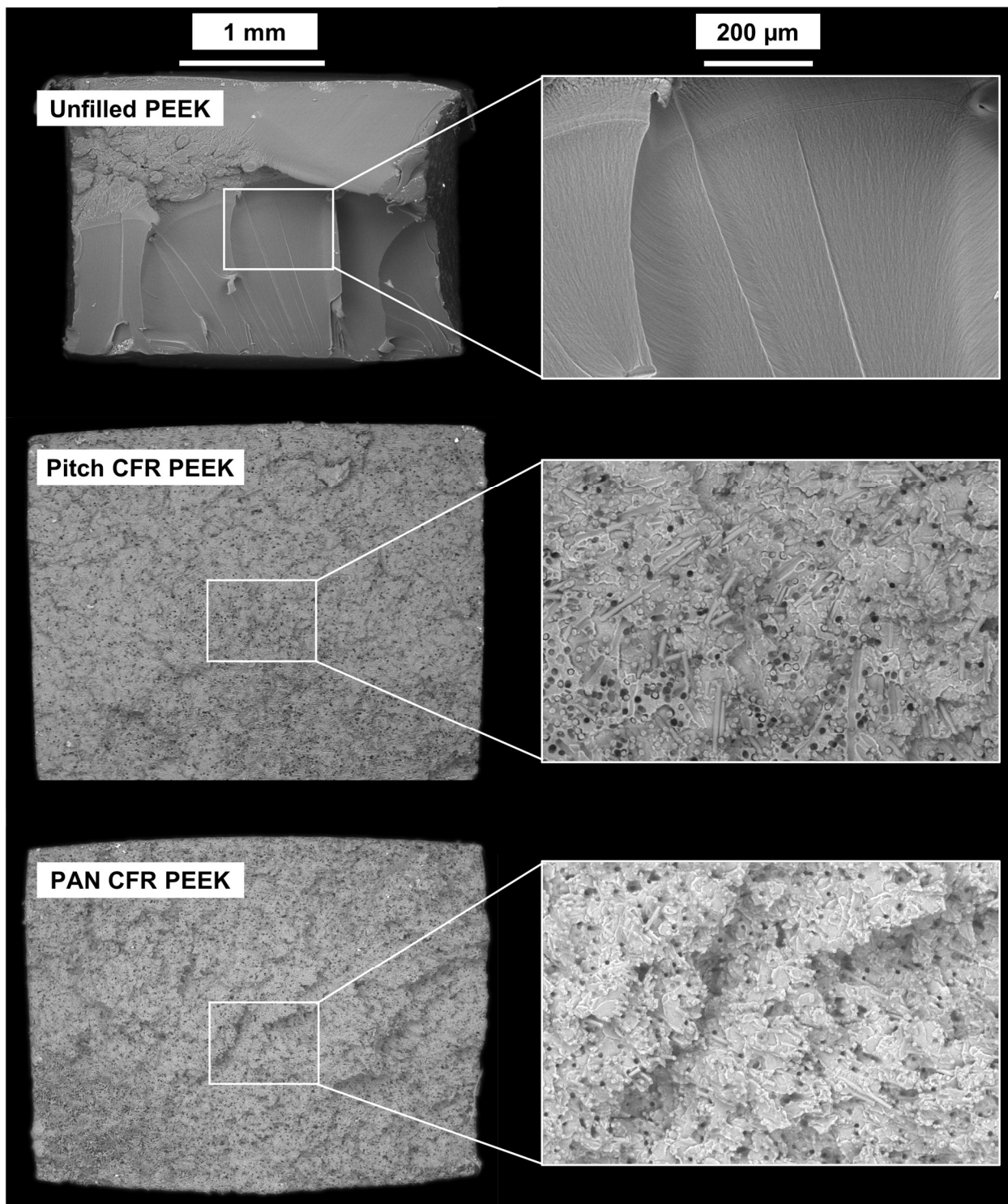
ΔK (MPa\sqrt{m}) at $da/dN = 2 \times 10^{-4}$ mm/cycle	
Unfilled	
0 °C	4.9
200 °C	5.0
300 °C	4.7
Pitch	
0 °C	4.7
200 °C	4.3
300 °C	4.8
PAN	
0 °C	5.7
200 °C	5.6
300 °C	7.0

470
471
472
473

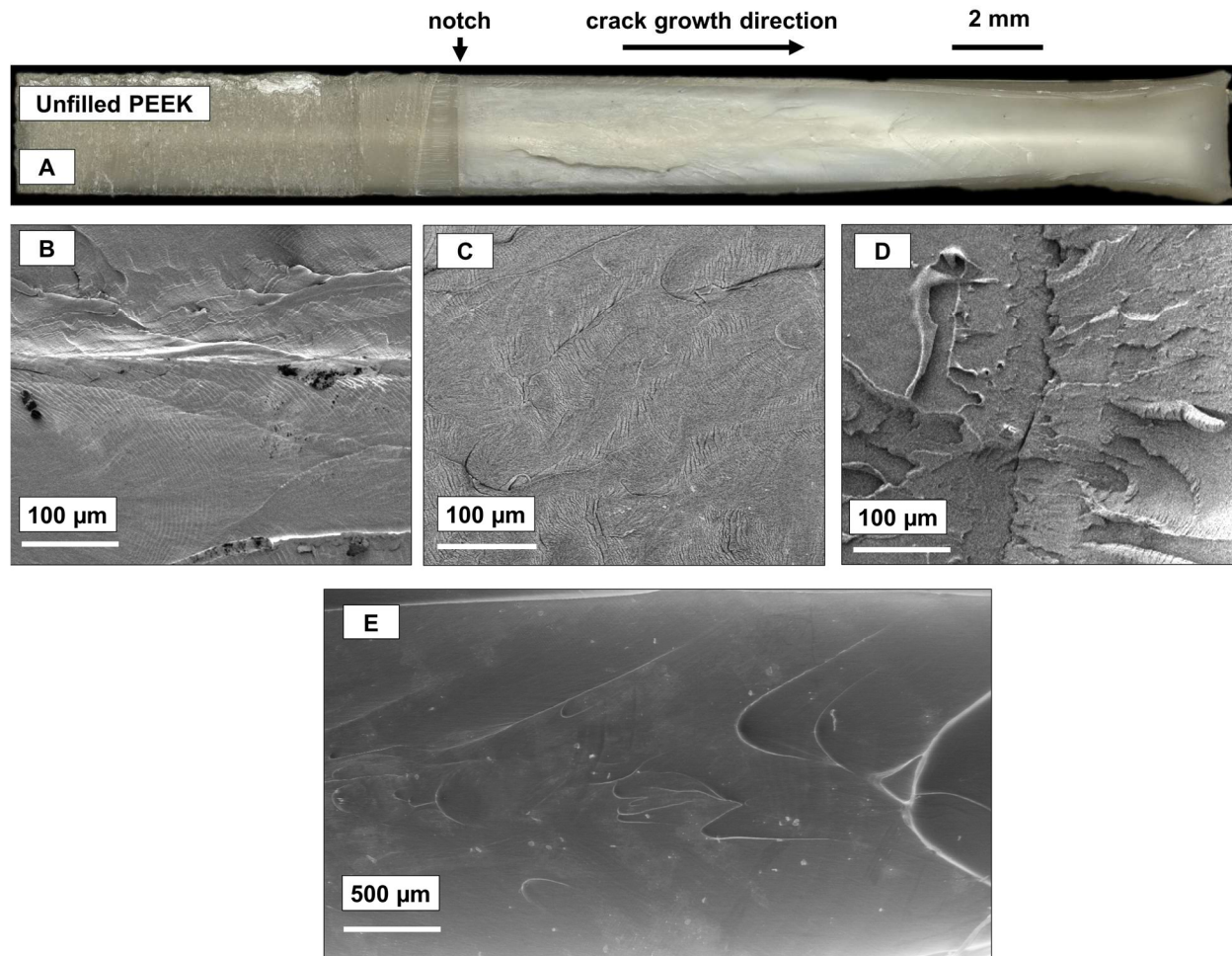


474
475
476

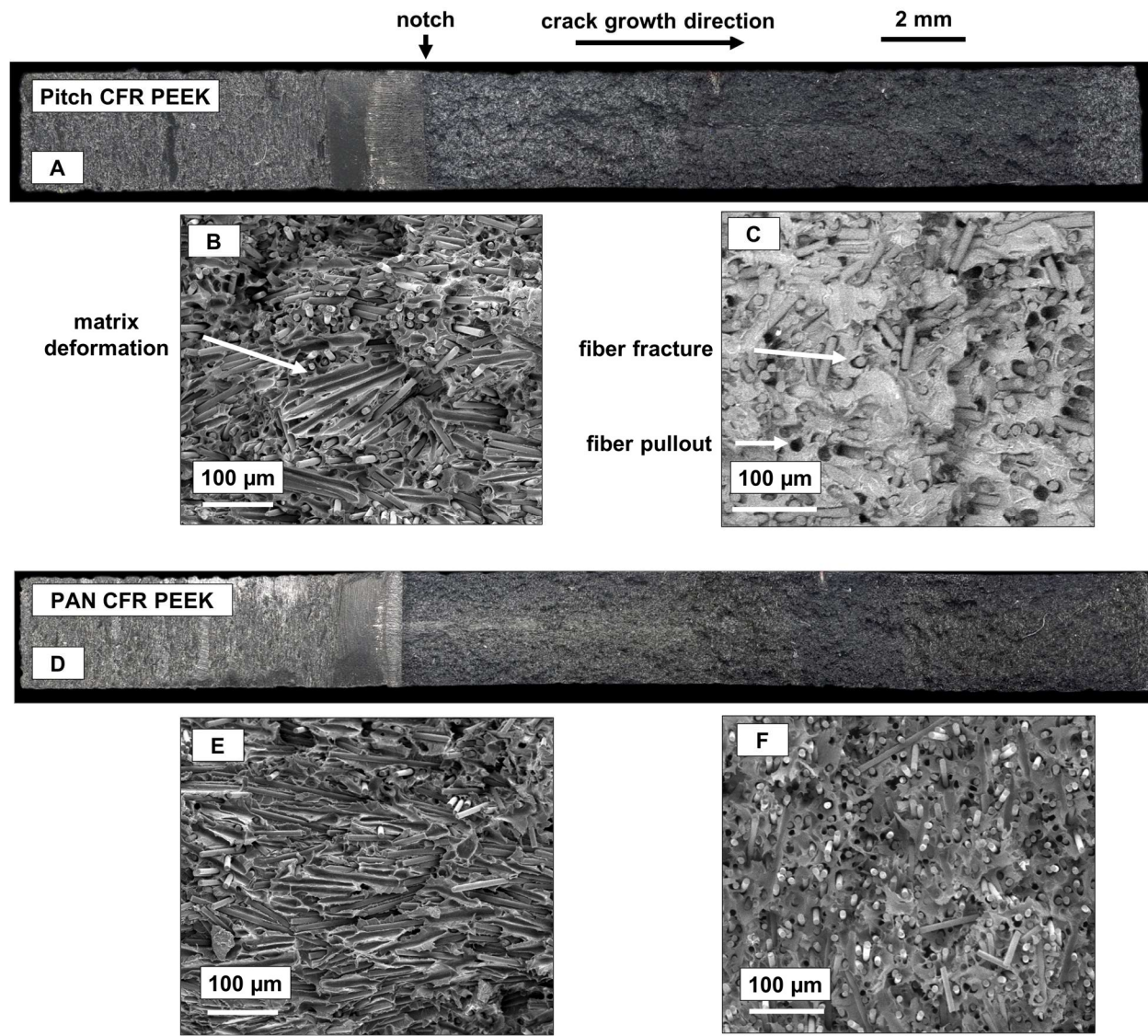
Figure 5. Paris constant, m, describing the rate of crack acceleration (slope of the da/dN versus ΔK plot) for all material formulations and heat-treatments.



477
478 Figure 6. SEM images of the fracture surfaces of monotonically tested samples (non-heat-treated
479 formulations).



480
 481 Figure 7. Images of the fracture surfaces of fatigue tested unfilled PEEK (non-heat-treated
 482 formulations). B: Early growth region. C: Mid growth region. D: Fast fracture region. E: Mid-
 483 to-late growth region.



484
 485 Figure 8. Images of the fracture surfaces of fatigue tested pitch (top) and PAN (bottom) CFR
 486 PEEK (non-heat-treated formulations). B and E: Early growth region. C and F: Fast fracture
 487 region.
 488

489 7. Acknowledgements

490 The authors would like to acknowledge Limacorporate SpA for material and manufacturing
491 support.

492 8. Bibliography

- 493 [1] Kurtz S. An Overview of PEEK Biomaterials. In: Kurtz S, editor. PEEK Biomaterials
494 Handbook. 2012. p. 1–7.
- 495 [2] Kurtz S, Devine J. PEEK biomaterials in trauma, orthopedic, and spinal implants.
496 *Biomaterials*. 2007;28(32):4845–69.
- 497 [3] Kumar S, Anderson D, Adams W. Crystallization and Morphology of Poly(aryl-ether-
498 ether-ketone). *Polymer (Guildf)*. 1986;27:329–36.
- 499 [4] Reitman M, Jaekel D, Siskey R, et al. Morphology and crystalline architecture of
500 polyaryletherketones. In: Kurtz S, editor. PEEK Biomaterials Handbook. 2012. p. 49–60.
- 501 [5] Green S, Schlegel J. A Polyaryletherketone Biomaterial for use in Medical Implant
502 Applications. In: Polymers for the Medical Industry, Proceedings of a Conference held in
503 Brussels. 2001. p. 1–7.
- 504 [6] Blundell D, Osborn B. The Morphology of Poly(aryl-ether-ether-ketone). *Polymer*
505 *(Guildf)*. 1983;24:953–8.
- 506 [7] Tung C, Dynes P. Morphological characterization of polyetheretherketone-carbon fiber
507 composites. *J Appl Polym Sci*. 1987;33:505–20.
- 508 [8] Mehmet-Alkan A, Hay J. The Crystallinity of PEEK Composites. *Polymer (Guildf)*.
509 1993;34(16):3529–31.
- 510 [9] Velisaris C, Seferis J. Heat Transfer Effects on the Processing-Structure Relationships of
511 Polyetheretherketone (PEEK) Based Composites. *Polym Eng Sci*. 1988;28(9):583–91.
- 512 [10] Ernstberger T, Buchhorn G, Heidrich G. Artifacts in spine magnetic resonance imaging
513 due to different intervertebral test spacers. *Neuroradiology*. 2008;51:525–9.
- 514 [11] Panfili E, Pierdicca L, Salvolini L, et al. Magnetic resonance imaging (MRI) artefacts in
515 hip prostheses: A comparison of different prosthetic compositions. *Radiol Medica*.
516 2014;119:113–20.
- 517 [12] Brantigan J, Steffee A. A Carbon Fiber Implant to Aid Interbody Lumbar Fusion: Two-
518 Year Clinical Results in the First 26 Patients. *Spine (Phila Pa 1976)*. 1993;18(14):2106–
519 17.
- 520 [13] Sastri V. High-Temperature Engineering Thermoplastics: Polysulfones, Polyimides,
521 Polysulfides, Polyketones, Liquid Crystalline Polymers, and Fluoropolymers. In: *Plastics*
522 *in Medical Devices*. 2nd ed. 2014. p. 173–213.
- 523 [14] Kurtz S. Applications of polyaryletheretherketone in spinal implants. In: Kurtz S, editor.
524 PEEK Biomaterials Handbook. 2012. p. 231–51.
- 525 [15] Rotini R, Cavaciocchi M, Fabbri D, et al. Proximal Humeral Fracture Fixation:
526 Multicenter Study with Carbon Fiber PEEK Plate. *Musculoskelet Surg*. 2015;99:1–8.
- 527 [16] Schliemann B, Hartensuer R, Koch T, et al. Treatment of Proximal Humerus Fractures
528 with a CFR-PEEK Plate: 2-year Results of a Prospective Study and Comparison to
529 Fixation with a Conventional Locking Plate. *J Shoulder Elb Surg*. 2015;1282–8.
- 530 [17] Akhavan S, Matthiesen M, Schulte L, et al. Clinical and histologic results related to a low-
531 modulus composite total hip replacement stem. *J Bone Jt Surg*. 2006;88:1308–14.

- 532 [18] Glassman A. Composite femoral stem for total hip arthroplasty. *Curr Opin Orthop*.
533 2008;19(1):6–10.
- 534 [19] Uthoff H, Poitras P, Backman D. Internal Plate Fixation of Fractures: Short History and
535 Recent Developments. *J Orthop Sci*. 2006;11:118–26.
- 536 [20] Bugbee W, Culpepper W, Engh C, et al. Long-Term Clinical Consequences of Stress-
537 Shielding After Total Hip Arthroplasty Without Cement. *J Bone Jt Surg*.
538 1997;79(7):1007–12.
- 539 [21] Reilly D, Burstein A. The elastic and ultimate properties of compact bone tissue. *J*
540 *Biomech*. 1975;8(6).
- 541 [22] Li C, Vannabouathong C, Sprague S, et al. The use of carbon-fiber-reinforced (CFR)
542 PEEK material in orthopedic implants: A systematic review. *Clin Med Insights Arthritis*
543 *Musculoskelet Disord*. 2014;8:33–45.
- 544 [23] Wang A, Lin R, Stark C, et al. Suitability and limitations of carbon fiber reinforced PEEK
545 composites as bearing surfaces for total joint replacements. *Wear*. 1999;225–229:724–7.
- 546 [24] Polineni V, Wang A, Essner A, et al. Characterization of Carbon Fiber-Reinforced PEEK
547 Composite for use as a Bearing Material in Total Hip Replacements. *ASTM Int*. 1998;266–
548 73.
- 549 [25] Regis M, Lanzutti A, Bracco P, et al. Wear behavior of medical grade PEEK and CFR
550 PEEK under dry and bovine serum conditions. *Wear*. 2018;408–409(May):86–95.
- 551 [26] Invibio. PEEK-OPTIMA Wear Performance: Typical Material Properties [Internet]. 2013
552 [cited 2016 May 2]. Available from: [https://invibio.com/ortho/materials/peek-optima-](https://invibio.com/ortho/materials/peek-optima-wear-performance)
553 [wear-performance](https://invibio.com/ortho/materials/peek-optima-wear-performance)
- 554 [27] Flock J, Friedrich K, Yuan Q. On the friction and wear behaviour of PAN-and pitch-
555 carbon fiber reinforced PEEK composites. *Wear*. 1999;225–229:304–11.
- 556 [28] Huang X. Fabrication and properties of carbon fibers. *Materials (Basel)*. 2009;2(4):2369–
557 403.
- 558 [29] Regis M, Fusi S, Favaloro R, et al. CFR PEEK composites for orthopaedic applications.
559 In: 9th International Conference on Composite Science and Technology. 2013.
- 560 [30] Yuan Q, Bateman S, Friedrich K. Thermal and mechanical properties of PAN- and pitch-
561 based carbon fiber reinforced PEEK composites. *J Thermoplast Compos Mater*.
562 2008;21(4):323–36.
- 563 [31] Sardar Z, Jarzem P. Failure of a Carbon Fiber-Reinforced Polymer Implant Used for
564 Transforaminal Lumbar Interbody Fusion. *Glob Spine J*. 2013;3(4):253–6.
- 565 [32] Tullberg T. Failure of a Carbon Fiber Implant. A Case Report. *Spine (Phila Pa 1976)*.
566 1998;23(16):1804–6.
- 567 [33] Ansari F, Chang J, Huddleston J, et al. Fractography and oxidative analysis of gamma
568 inert sterilized posterior-stabilized tibial insert post fractures: Report of two cases. *Knee*.
569 2013;20(6):609–13.
- 570 [34] Tower A, Currier J, Currier B, et al. Rim Cracking of the Cross-Linked After Total Hip
571 Arthroplasty. *J Bone Jt Surg*. 2007;2212–7.
- 572 [35] Bonnheim N, Gramling H, Ries M, et al. Fatigue fracture of a cemented Omnifit CoCr
573 femoral stem: implant and failure analysis. *Arthroplast Today*. 2017;3:234–8.
- 574 [36] Saib K, Isaac D, Evans W. Effects of processing variables on fatigue in molded PEEK and
575 its short fiber composites. *Mater Manuf Process*. 1994;9(5):829–50.
- 576 [37] Saib K, Evans W, Isaac D. The role of microstructure during fatigue crack growth in poly
577 (aryl ether ether ketone) (PEEK). *Polymer (Guildf)*. 1993;34(15):3198–203.

- 578 [38] Brillhart M, Botsis J. Fatigue crack growth analysis in PEEK. *Int J Fatigue*. 1994;16:134–
579 40.
- 580 [39] Brillhart M, Botsis J. Fatigue fracture behavior of PEEK: 2. Effects of thickness and
581 temperature. *Polymer (Guildf)*. 1992;33(24):5225–32.
- 582 [40] Brillhart M, Gregory B, Botsis J. Fatigue fracture behavior of PEEK: 1. Effects of load
583 level. *Polymer (Guildf)*. 1991;32(9):1605–11.
- 584 [41] Karger-Kocsis J, Walter R, Friedrich K. Annealing effects on the fatigue crack
585 propagation of injection-moulded PEEK and its short fibre composites. *J Polym Eng*.
586 1988;8(3–4):221–53.
- 587 [42] Chu J, Schultz J. The influence of microstructure on the failure behaviour of PEEK. *J*
588 *Mater Sci*. 1990;25:3746–52.
- 589 [43] Friedrich K, Walter R, Voss H, et al. Effect of short fibre reinforcement on the fatigue
590 crack propagation and fracture of PEEK-matrix composites. *Composites*. 1986;17(3):205–
591 16.
- 592 [44] Evans W, Isaac D, Saib K. The effect of short carbon fibre reinforcement on fatigue crack
593 growth in PEEK. *Composites*. 1996;27A:547–54.
- 594 [45] Regis M, Zanetti M, Pressacco M, et al. Opposite role of different carbon fiber
595 reinforcements on the non-isothermal crystallization behavior of poly(etheretherketone).
596 *Mater Chem Phys*. Elsevier B.V; 2016;179:223–31.
- 597 [46] Regis M, Bellare A, Pascolini T, et al. Characterization of thermally annealed PEEK and
598 CFR-PEEK composites. *Polym Degrad Stab*. 2017;136:121–30.
- 599 [47] Maksimov R, Kubat J. Time and temperature dependent deformation of poly(ether ether
600 ketone) (PEEK). *Mech Compos Mater*. 1997;33(6):517–25.
- 601 [48] Ansari F. The Interplay of Design and Materials in Orthopedics: Evaluating the Impact of
602 Notch Geometry on Fatigue Failure of UHMWPE Joint Replacements. Dissertation, UC
603 Berkeley. 2015.
- 604 [49] Invibio. PEEK-OPTIMA Natural: Typical Material Properties [Internet]. 2013 [cited 2016
605 Apr 18]. Available from: [https://invibio.com/library?id=%7B9ec81b92-8ab8-40da-af8f-
606 6c3bf002aa84%7D](https://invibio.com/library?id=%7B9ec81b92-8ab8-40da-af8f-6c3bf002aa84%7D)
- 607 [50] Invibio. PEEK-OPTIMA Reinforced: Mechanical Properties, Physical Properties and
608 Biocompatibility [Internet]. 2014 [cited 2016 Apr 18]. Available from:
609 <https://invibio.com/library?id=%7B4957faed-3d7d-466b-bed0-f8dfcf1a6e5a%7D>
- 610 [51] Lafdi K, Wright M. Carbon fibers. In: Peters S, editor. Handbook of Composites. London:
611 Chapman & Hall; 1998. p. 169–201.
612